

8900811

CNIC-00193

SJU-0001

中国核科技报告

CHINA NUCLEAR SCIENCE & TECHNOLOGY REPORT

二维逆环状流膜态沸腾传热数学解析模型



中国核情报中心

China Nuclear Information Centre

CNIC-00193

SJU-0001

二维逆环状流膜态沸腾传热数学解析模型

徐济鋈 杨燕华 陈 枫

(上海交通大学)

中国核情报中心

北京·1988.4

摘 要

作者根据逆环状流膜态沸腾 (IAFB) 的可视化实验结果,将该流型理想化为一个两区物理模型。按双区物理模型假定,建立二维、二流体数学解析模型。它由质量、动量和能量守恒微分方程以及相应的本构方程构成完全方程组,然后用数值方法求解。用该模型分析了液相、汽相参数以及加热管的壁温,与Stewart的实验数据进行了比较,两者相当一致。可信地预示了液体过冷度、质量流率、系统压力和加热热流率对加热面温度的影响。同时选择实例分析了流动二维效应和初始汽膜厚度取值对加热面温度和膜厚变化的影响。结果表明:在讨论的范围内忽略二维效应对壁面温度影响不大;初始膜厚取值不同对加热面温度变化和膜厚变化无显著影响。

关键词 膜态沸腾 安全分析 反应堆 数学模型

TWO-DIMENSIONAL ANALYTICAL MODEL OF INVERTED-ANNULAR FILM BOILING

Hsu Chichun Yang Yanhua Cheng Feng

(Shanghai Jiao Tong University)

ABSTRACT

A two-dimensional two-fluid model is developed to predict the liquid and vapour parameters as well as the surface temperature of a heated tube. A two regions of physical modeling represents inverted-annular film boiling (IAFB) based on author's visual observations. The analytical model is consisted of a set of differential conservation equations together with appropriate closure correlations and solved numerically. Successful comparisons are made between model predictions and Stewart's experimental data. Generally, the model predicts correctly the dependence of wall temperature on liquid subcooling, mass flow rate, pressure and heat flux input. The two dimensional effectness isn't very significant. The initial vapour film thickness doesn't influence the wall temperature predictions very much.

1. Introduction

Inverted-annular film boiling is usually encountered in accident analysis of nuclear reactors during the reflooding phase following a postulated loss-of-coolant accident (LOCA). A good understanding of the heat transfer processes occurring is of paramount importance for the determination of the peak cladding temperature. It is also important for many other areas of engineering technology and geophysics such as the cooling of rocket engines, quenching of metals and flow of cryogenic liquids in heated pipes.

The two-phase flow and heat transfer phenomena in IAFB are rather complex. The heat is transferred from the hot wall to the vapour blanket and subsequently from the vapour to the liquid core. Some heat will also be transferred directly from wall to the liquid core by radiation. For a initial subcooled liquid core, part of this heat will be used for raising the vapour temperature and part for reducing the subcooling. For a saturated liquid core, the heat will be mainly for vaporization, hence rapidly increasing the vapour film thickness. All these heat transfer mechanisms are not well understood. The presence of waves on the liquid-vapour interface causes the mechanisms more complication. A brief review of film boiling correlations and analytical models available has been made by Analytis and Yadigaroglu⁽¹⁾. The conclusion is that almost all the models cannot predict the experimental findings of strong dependence of the heat transfer coefficient on reflooding velocity, subcooling and pressure observed and an appropriate two-fluid model of the IAFB seems to be the only way of properly approaching this problem.

In recent years, several two-fluid models simulated to the IAFB have been postulated. The theoretical model by Elias and Chambre⁽²⁾ only solved the entrance-region problem for the vapour film based on the energy conservation equation. The thickness of the vapour film, which is important for IAFB heat transfer, left as adjustable parameter. In the annular vapour space a uniform (constants) velocity profile is assumed. An empirical correlation for the film thickness is extracted from experimental data. Fung and Groeneveld⁽³⁾ used an one-dimensional integral technique by considering a development of the thermal boundary layers both in the liquid core and in the vapour film. The liquid core is assumed to be in turbulent flow and the velocity profile of the core is assumed uniform. The model predicts correctly the effects of flow, inlet subcooling and axial location on wall temperatures.

Analytis and Yadigaroglu⁽¹⁾ also developed a two-fluid model which is an improved version of the earlier two-fluid model of Chan and Yadigaroglu. A frame of reference moving with the quenching front is used. A set of six differential conservation equations solved numerically. The model predicts correctly the dependence of the heat transfer coefficient on liquid subcooling and flow rate. For some cases, heat transfer is still under-predicted. All the aforementioned models are essentially one dimensional. In practice, it seems to be a thermal entrance region problem in the downstream from the quenching front, i.e. in post-CHF region. The two dimensional effects may be important in some cases. The present paper is dealing with a two-dimensional, two-region, two-fluid analytical model of IAFB.

2. Physical Model

2.1 Visual Experiments

Systematic visual observations of IAFB carried out at author's university have indicated the effects of subcooling, heat flux and mass flow rate on the vapour film behavior⁽⁴⁾. Three typical photographs of IAFB shown in Fig.1 were taken at the inlet subcoolings 6°C, 14°C and 31°C, respectively. A constant thickness film is occurred starting from the DNB point following by a wavy developing and film thickening vapour blanket taking place at some downstream section shown in Fig.1.C. In Fig.1,b the constant thickness range is much shorter and in Fig.1.a there is on obvious constant thickness range. Two distinct regions of IAFB existed also have been indicated by Elias and Chamber⁽²⁾. The first region occurs immediately above the quenching front and is characterized by a smooth vapour film of constant thickness separating the bulk liquid phase from the hot wall. In the second region taking place further downstream, a wavy and unstable vapour-liquid interface is observed. The constant film thickness means the vapour is entirely generated in the entrance section or DNB section and the corresponding interface temperature is slightly subcooled locally. The unstable vapour liquid interface and thickening blanket imply that the evaporation is generated up beyond some transition section which can be regarded as the saturation temperature of the liquid has been reached. Whether the first region occurs is dependent on the inlet subcooling, heat flux input and flow rate. Generally, for low subcooling and near saturated conditions only second region is developed.

2.2 Schematic Model

A schematic representation of two-regions model of the IAFB is formulated in Fig.2.

Actually, the film thickness is slightly increased with vapour heated up. The thickness variation, however, is minor. But for the second region beyond the interfacial saturation section the thickness is rapidly increased with vaporization from liquid-vapour interface. A part of the heat input will be used to heat up vapour and part for reducing subcooling if the first region occurs. Part of the heat will be used for heating the vapour and part for vaporization of liquid core. So the present two-regions model is rather emphasized on thermohydrodynamics unlike a pure geometrical representation. But the interface of liquid-vapour is assumed smooth and the film width is variable. The following assumptions are made in order to obtain simplified form of the conservation equations.

(1) For the vapour-liquid interface, evaporation only occurs in second region and the phase change is negligible in first region.

(2) A vapour film is completely separated from the liquid core and no entrainment in each other is considered.

(3) The annular film and the liquid column are both considered axial symmetry.

(4) Neglect of pressure difference at the two sides of the interface due to the presence of a vapour thrust force. The pressures applied on both phases are equal.

(5) The vapour film and the liquid column are both in turbulent.

(6) No radiation heating for the vapour film.

(7) The flow is steady.

3. Analytical Model

As mentioned above, the vapour blanket is expanding as the flow advances and heat input whatever in first or second region. A reducing liquid column together with a expanding vapour blanket which causes the velocity profile changeable both in vapour film and in liquid core, hence, which will affect temperature profile. It seems to be a thermal entrance region problem. A two dimensional effect may be significant. A two-dimensional, two-region and two-fluid analytical model have to be studied.

3.1. Conservation Equations

In a frame of two-dimension, two-region, two-fluid model, the mass, momentum and energy conservation equations for the liquid column and vapour blanket will be

$$\frac{\partial}{\partial z}(\rho V_z) + \frac{1}{r} \frac{\partial}{\partial r}(\rho r V_r) = 0 \quad (1)$$

$$\rho V_r \frac{\partial V_z}{\partial r} + \rho V_z \frac{\partial V_z}{\partial z} = -\frac{dp}{dz} - \rho g + \frac{1}{r} \frac{\partial}{\partial r} (\mu r \frac{\partial V_z}{\partial r}) \quad (2)$$

$$\rho C_p (V_r \frac{\partial T}{\partial r} + V_z \frac{\partial T}{\partial z}) = \frac{1}{r} \frac{\partial}{\partial r} (K r \frac{\partial T}{\partial r}) \quad (3)$$

In the derivation of these equations the viscous dissipation and several comparative smaller terms are neglected. A. phase change equation is

$$\frac{d}{dz} \int_0^{R_1} \rho_l V_z 2\pi r dr = -\Gamma, \quad (4)$$

$$\frac{d}{dz} \int_{R_1}^R \rho_v V_z 2\pi r dr = \Gamma, \quad (5)$$

Where subscripts v for vapour, l for liquid. Integrating of equation (4) and (5) then added

$$\int_0^{R_1} \rho_l V_z 2\pi r dr + \int_{R_1}^R \rho_v V_z 2\pi r dr = W = \text{total mass flow rate}$$

3.2 Boundary Conditions

The boundary conditions in wall surface will be

$$\begin{aligned} V_r|_{r=R} &= 0 \\ V_z|_{r=R} &= 0 \\ (K \frac{\partial T}{\partial r})|_{r=R} &= q_w - q_R \end{aligned} \quad (6)$$

Here q_R for radiation heat flux component, q_w , for total heat flux.

In the interface

$$\begin{aligned} V_{z,v}|_{r=R_1} &= V_{z,l}|_{r=R_1} \\ (\mu \frac{\partial V_z}{\partial r})|_{r=R_1} &= (\mu \frac{\partial V_z}{\partial r})|_{r=R_1} \\ T_v|_{r=R_1} &= T_s \end{aligned} \quad (7)$$

$$\Gamma_s = \frac{2\pi R_1}{H_{i0}} \left[(K \frac{\partial T}{\partial r})|_{r=R_1} - (K \frac{\partial T}{\partial r})|_{r=R_1} + q_R \frac{R}{R_1} \right]$$

In the interface of liquid side, the heat transferred into liquid is used exclusively to reduce the subcooling in the first region

$$(K \frac{\partial T}{\partial r})|_{r=R_1} = (K \frac{\partial T}{\partial r})|_{r=R_1} + q_R \frac{R}{R_1} \quad (8)$$

For second region by the assumption the interface is in saturation

$$T|_{r=R_1} = T_s \quad (8a)$$

In the centre of liquid column, ($r=0$)

$$V_r|_{r=0} = 0$$

$$\left. \frac{\partial V_x}{\partial r} \right|_{r=0} = 0 \quad (9)$$

$$\left. \frac{\partial T}{\partial r} \right|_{r=0} = 0$$

3.3 Initial Conditions

Provided the initial values of the variables are known at DNB section and some relationships are specified, the conservation equations can be solved by finite differential method.

3.3.1. temperature and mass flow rate

Following Elias the initial temperature profile will be

$$T_v(r, 0) = T_s \quad (10)$$

The initial flow rates of vapour film and liquid column, respectively

$$W_{v,0} = \frac{Q_{Hv}}{H_s - H_l} \quad (11)$$

$$W_{l,0} = W - W_{v,0}$$

where Q_{Hv} is part of heat for generating saturated steam at hot patch. If Q_{Hl} is the total heat input to hot patch, then

$$H_{l,0} = H_l + \frac{Q_{Hl} - Q_{Hv}}{W_{l,0}} \quad (12)$$

$$T(r, 0) = T_{l,0} = f(H_{l,0})$$

3.3.2. Velocity profile

Usually, the flow is fully-developed before the DNB section. The initial velocity profile of liquid column is assumed uniform (constant)

$$V_{z,l}(r, 0) = V_{z,l,0} = \frac{W_{l,0}}{\rho_{l,0} \pi R_0^2} \quad (13)$$

R_0 , initial radius of liquid column. In general, initial vapour film is in laminar.

Assumption of parabolic profile will be adopted

$$V_{z,v}(r, 0) = A_2(R-r)^2 + A_1(R-r) \quad (14)$$

Where
$$A_2 = \frac{2V_{z,l,0} \rho_v \delta_0 (3R - 2\delta_0) - 6W_{v,0}}{\rho_v \delta_0^2 (2R - \delta_0)}$$

$$A_1 = (V_{z,l,0} - A_2 \delta_0^2) / \delta_0$$

Initial film thickness δ_0 is $R - R_0$, which is calculated by phase change equation. The dependence of wall temperature on δ_0 isn't significant. This will be shown in the following section.

3.3.3 initial mass fraction of vapour

The equilibrium steam quality $X_{e,0}$ and actual quality $X_{a,0}$ will be

$$X_{e,0} = (H_l + \frac{Q_H}{W} - H_l) / H_{l,0} \quad (15)$$

$$X_{s,0} = W_{v,0}/W$$

And the quality variables will be

$$X_s(z) = X_{s,0} + \frac{q_s \cdot z}{W \cdot H_{fg}} \quad (16)$$

$$X_s(z) = X_{s,0} + \frac{1}{W} \int_0^z \Gamma_s(z) dz \quad (17)$$

for uniform heating. Actual void fraction $\alpha(z)$

$$\alpha(z) = 1 - \frac{R_s^2}{R^2} \quad (18)$$

3.4 Constitutive Equations

In order to obtain a complete set of equations, the constitutive equations for viscosity and conductivity have to be specified.

$$\begin{aligned} \mu &= \mu_L + \epsilon_m \cdot \rho \\ k &= k_L + \epsilon_k \cdot \rho C_p \end{aligned}$$

Where μ_L and k_L for laminar viscosity and laminar conductivity ϵ_m and ϵ_k for momentum eddy diffusivity and energy eddy diffusivity, respectively. The former two are dependent on local temperature and pressure conditions. The

latter two depend on local hydrodynamics and locations. Using Prandtl mixing length hypothesis, the eddy diffusivity for momentum transfer is given by

$$\epsilon_m = cl(\bar{V}_{z,m,z} - \bar{V}_{z,m,0})$$

here l is mixing zone width and c is a proportionality constant. Following Fung's assumption⁽¹¹⁾, the mixing zone width is defined to be half of the turbulent vapour film thickness $\frac{\delta(z)}{2}$. In addition, the velocity difference is assumed to be proportional to the average liquid velocity $\bar{V}_{z,l}$. Hence

$$\epsilon_m = c_1 \left(\frac{1}{2} \delta\right) \bar{V}_{z,l} \quad (19)$$

For vapour film, the mixing length is assumed to be proportional to a distance between location and wall surface.

$$\epsilon_{m,v} = c_v (R-r) \bar{V}_{z,v} \quad (20)$$

For the eddy diffusivity of heat, the turbulent Prandtl number Pr_t is suggested by

$$Pr_t = \epsilon_m / \epsilon_k$$

By assuming that Reynolds' analogy is valid, $Pr_{t,l} = 1$. For vapour film a Webb's modified correlation⁽⁶⁾ is used

$$Pr_{t,v} = \frac{1 + 57 Re_v^{-0.46} \cdot Pr_v^{-0.65} \cdot \exp\left[-\left(\frac{R-r}{R}\right)^{\frac{1}{2}}\right]}{1 + 135 Re_v^{-0.46} \cdot \exp\left[-\left(\frac{R-r}{R}\right)^{\frac{1}{2}}\right]} \quad (21)$$

For simplicity, c_1 is 0.08 taken from Fung analysis. Based on Stewart's data⁽⁶⁾ $Pr_{t,v}$ will be located between 0.55~0.65, hence 0.6 is used for analysis.

The adjusting factor c_v is approximate to 0.17. Hence the constitutive correlations will be

$$\begin{aligned}\mu_1 &= \mu_{L1} + 0.04 \delta \cdot \bar{V}_{z1} \rho_1 \\ k_1 &= k_{L1} + 0.04 \delta \cdot \bar{V}_{z1} \rho_1 C_{p1} \\ \mu_v &= \mu_{L1} + 0.017(R-r) \bar{V}_{zv} \cdot \rho_v \\ k_v &= k_{L1} + 0.0283(R-r) \bar{V}_{zv} \cdot \rho_v \cdot C_{pv}\end{aligned}\quad (22)$$

3.5. Heat flux correlations

A realistic modeling of the different heat transfer mechanisms is of paramount importance for the development of a mechanistic model of IAFB. In state of the art, these mechanisms are not well-understood. This is an open research area. Following previous analysis and by assumption of 6, the wall radiation heat flux is evaluated by assuming radiation exchange between the tube wall and the liquid core, with an absorbing medium in between.

$$q_{rx} = \frac{\sigma_{sb}}{\frac{1}{\epsilon_w \sqrt{1-\alpha}} + \left(\frac{1}{\epsilon_l} - 1\right)} [(T_w + 273.15)^4 - (T_{l|_{r=R_1}} + 273.15)^4] \quad (23)$$

Where σ_{sb} ; Stefan-Boltzman Constant, ϵ emissivity.

The existence of random disturbances on the liquid-vapour interface may result in intermittent touching of the liquid with the wall surface. In Edelman observations^[7], the wall of entrance region rewetted is significant. The rewet probability may be high to 80% following an exponential decay downstream of the DNB, which may depend on subcooling.

Hence a modified term considering rewet is added to correlation (22).

$$k_v = k_{L1} + \epsilon_v \rho_v C_{pv} + c_1 [\exp(c_2 (T_s - T_{l|_{r=R_1}})) - 1] \cdot k_{L1}$$

With Stewart data $c_1 = c_2 = 0.05$ will be used.

For subcooled liquid, the IAFB regime will terminate at a certain distance. The breakdown mechanism is still not available. There are several option presented in papers. Groeneveld took void fraction of 30% as breakdown criterion. Analytis and Yadigaroglu assume the breakdown due to the development of large-amplitude interfacial waves and based on a critical Weber number. The critical Weber number is also unknown exactly now. An assumption of the centre of liquid core reaching at saturation temperature is adopted, at which bulk boiling of liquid column will be taken place and will break up it. We stipulate that all vapour properties are to be evaluated at the local film temperature $T_f(z)$

4. Wall Temperature Predictions and Comparison.

To assess the predictive capabilities and limitation of the model, we

choose a number of cases from Stewart data⁽⁶⁾, which cover a range of pressure (2,3,4 MPa), mass velocity [210~295kg/(m²·s)] heat flux input (120~250kW/m²) and inlet subcooling (12~46°C). The wall temperature predictions are well agreed with data in most cases. Detailed comparisons can be found in Chen's thesis. For 188 data, the average absolute deviation is about 13°C, the relative one about 2.27%. In Fig 3 some typical results are shown. The solid curves are for wall temperature predictions, the discreted points for Stewart's data. Fig.4 is for radial velocity profile and temperature profile at 0.4 m section from DNB point. Both profiles in vapour blanket vary drastically due to less viscosity and less conductivity, respectively.

A dependence of heat flux and subcooling on vapour film thickness is shown in Fig.5. In first region the thickness is nearly constant or increased gradually. For second region the thickness increases rapidly due to evaporation which agrees with visual observations.

The theoretical model does not take into consideration the inception of DNB. It is not certain how this would affect the radial temperature profile of the liquid core. The effects of various initial film thickness assumed are shown in Fig.6, only an initial disturbance exist and decays rapidly. Beyond 3cm axial distance no obvious difference is observed for thickness, the same results for wall temperature. Hence the effect of initial condition on wall temperature may be a local phenomenon and appear within a rather short range downstream from DNB point.

The authors also evaluate the two dimension effect for an arbitrary case. The comparison tells us less effect for first region (absolute deviation less about 1.5°C, relative one 0.25%), and that the effect in second region is a bit larger (absolute deviation; 6°C, relative; 0.8%). The wall temperature is a bit higher if the radial velocity component is omitted. As regarding the several adjusting factors, the authors believe no serious error will be induced if the radial velocity component is negligible. Thus an advantage of reducing computation expenses will be achieved.

5. Conclusion

1. A two-dimensional, two-regions and two-fluid model was developed to predict the surface temperature of a tube during IAFB. The dependences of wall temperature on various parameters are evaluated. The predictions compared well with Stewart's data.

2. To account for the effect of two-dimension an evaluation of one-dimension was performed. The less effect for first region, and a bit higher for

second region were shown. Neglecting the two-dimensional effect tends to conservation for wall temperature predictions.

3. The initial condition may influence the wall temperature within a short range downstream from DNB point. No influence was shown for film thickness predictions beyond this short range.

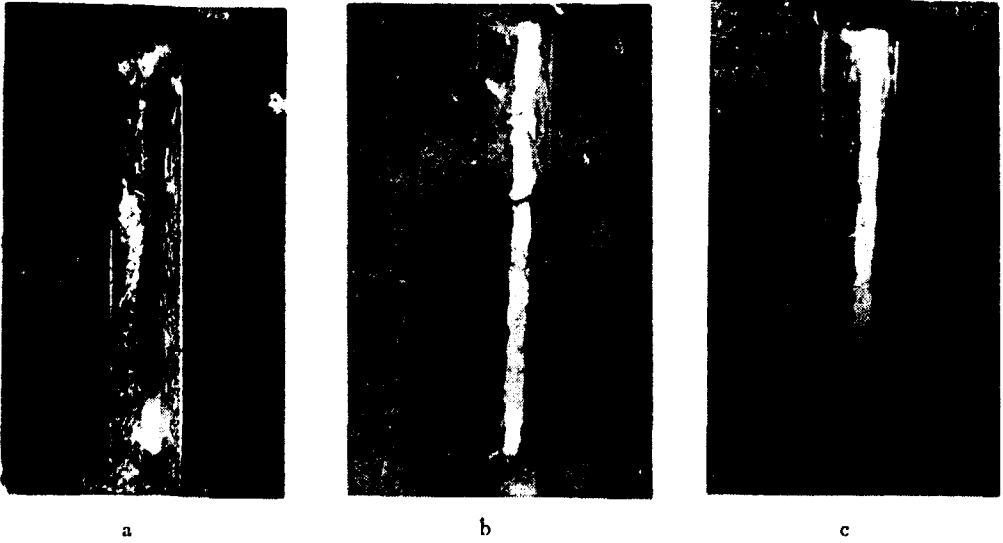


Figure 1. Typical film patterns as inlet subcoolings
 a, 6°C b, 14°C c, 31°C

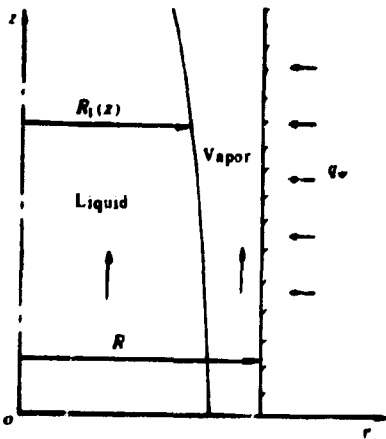


Figure 2. Schematic two regions model

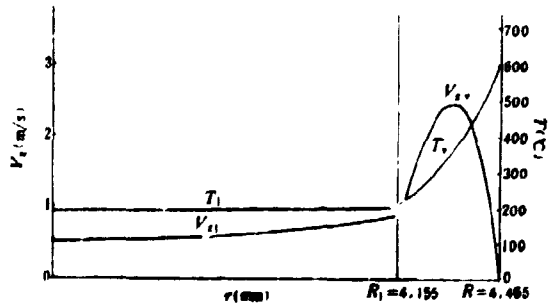


Figure 4. Radial velocity profile and temperature profile at 0.4m

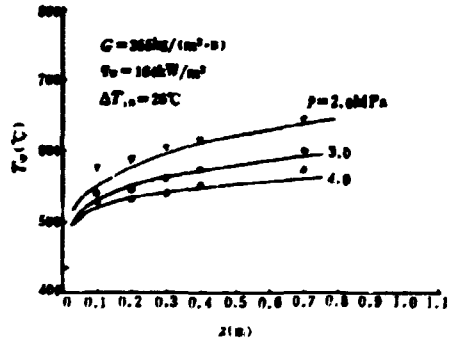
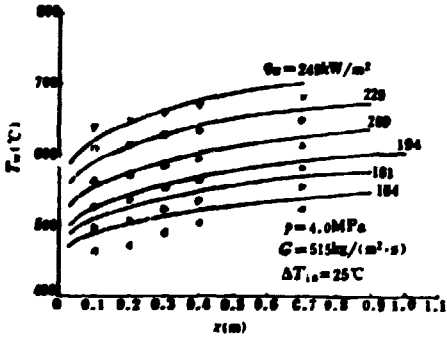
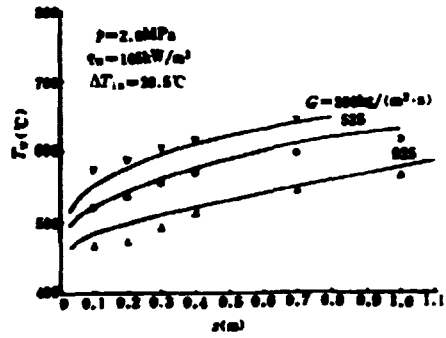
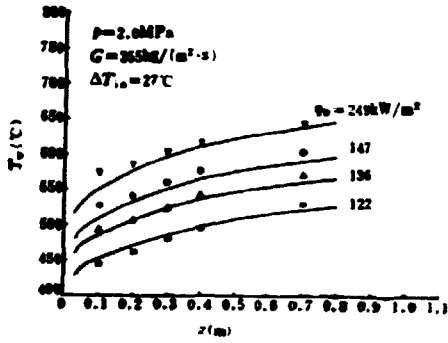


Figure 3. The predictions of wall temperature dependence of: a. heat flux, b. mass velocity, c. subcooling d. pressure

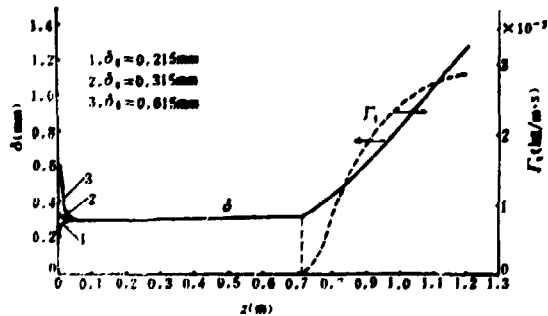


Figure 6. Initial film thickness effect

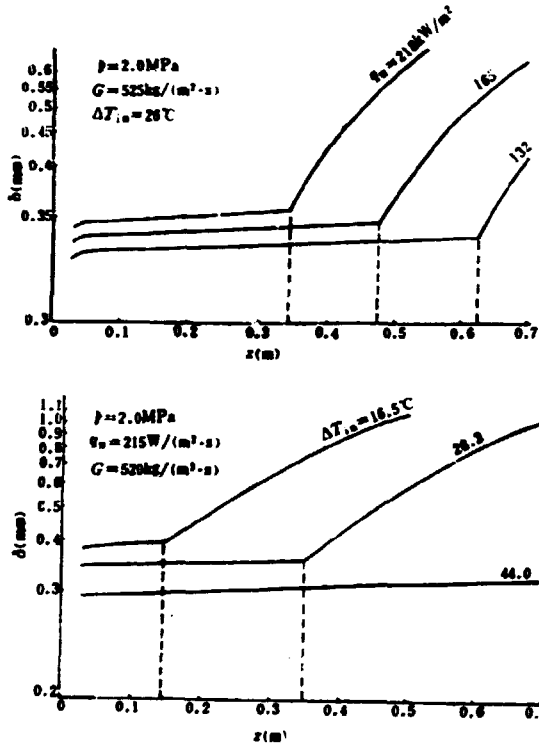


Figure 5. Dependence of heat flux and subcooling on film thickness

REFERENCES

- [1] G.Th.Analytis and G.Yadigaroglu, Analytical Modeling of Inverted Annular Film Boiling, Nucl. Engrg.and Des.99 (1987) 201-212
- [2] E.Elias and P.Chambre, Inverted-annular Film Boiling Heat Transfer from Vertical Surfaces. Nucl.Engrg.and Des.64 (1981) 249-257
- [3] K.K.Fung and D.C.Groeneveld, A Physical Model of Subcooled and Low Quality Film Boiling of Water in Vertical Flow at Atmospheric Pressure, Proceedings of the 7th International Heat Transfer Conference
- [4] Hsu Chi-Chun et.al.Low Pressure and Subcooled Water Flow Film Boiling Research by Visual Method.Presented on 4th Miami International Symposium on Multi-phase Transport and Particulate Phenomena, 15-17 Dec.1988.Miami Beach, Florid, U.S.A.
- [5] W.S.Webb and J.C.Chen, A Numerical Method for Turbulent Nonequilibrium Dispersed Flow Heat Transfer, Int.J.Heat Mass Transfer, Vol 25 (3) (1982)
- [6] J.C.Stewart and D.C.Groeneveld,Low-quality and Subcooled Film Boiling of Water at Elevated Pressures, Nucl.Engrg.and Des.67 (1981) 259-272
- [7] Z.Edelman et.al., Inverted Annular Boiling in a Stainless-steel Tube with Steady Heat Sources, Int.J.Heat Mass Transfer.Vol 28 (1983)
- [8] Cheng Feng, Subcooling Film Boiling Heat Transfer Research, M.SC.Thesis,Shanghai Jiao Tong University China, Feb.1987

一、引言

水冷反应堆失水事故 (LOCA) 的再淹没阶段常常会形成逆环状流膜态沸腾 (IAFB) 传热工况, 因而清晰了解它的传热机理对确定事故下元件包壳最大表面温度至关重要。不仅如此, 在其它工程领域和地球物理方面, 逆环状流膜态沸腾也获得了广泛应用。例如: 火箭发动机冷却, 金属淬冷和热管内制冷液体流动等等。

IAFB工况下的流动和传热现象相当复杂。热量首先由加热面传给汽膜而后再经蒸汽传递给液芯。同时, 在高温下炽热加热面经辐射换热直接加热液芯。如果初始段液芯处于过冷状态, 则液芯接受的热量主要用于减少过冷度, 与此同时蒸汽膜温度升高。如果液芯处于饱和状态, 则总加热热流中除少量用于升高汽膜蒸汽温度外, 主要部分使液芯汽化。这种情况下, 同时伴随汽膜迅速增厚。无论是液芯处于过冷状态或饱和状态, 上述传热过程机理至今了解不多。不仅如此, 实际上汽膜和液芯之间的交界面呈波状, 波动交界面使传热过程更为复杂。Analytis和Yadigaroglu曾讨论了已发表的一些(少量)分析模型, 他们认为实验表明 IAFB 下传热系数与再淹没速度、液体过冷度和系统压力之间存在着强的相依关系, 而几乎所有模型无法预示, 必须发展一个合适的两流体模型。

近年来, 已经发表了几个模拟IAFB的两流体模型。Elias 和 Chambre^[2]的模型假定蒸汽膜厚度为定值, 汽膜内速度分布不变且为定值, 建立IAFB的初始段能量守恒方程。令汽膜厚度作为拟合加热面温度测量值的可调整参数, 获得建立在实验基础上的膜厚经验式。Fung和Groeneveld^[3]将热边界层概念同时应用于蒸汽膜和液芯, 假定液芯为紊流, 其速度分布不变, 用一维积分方法求解守恒方程组, 模型合理地预示了流量、入口过冷度对壁温的影响, 以及预示了壁温沿轴向的变化。Analytis和Yadigaroglu^[1]的改进两流体模型, 将方程坐标建立在淬冷面(即将DNB截面作为运动坐标), 采用数值方法解6个守恒微分方程(式)组, 模型可以准确地预示传热系数对液体过冷度和流量的相依性。但是, 在某些工况下模型估计值偏小。上述所有分析模型都是一维的, 实际上临界热流密度后的逆环状流膜态沸腾发生在淬冷前沿的下游区, 急剧的相变过程使IAFB呈一种热入口区问题。可以推测在某些工况下流动二维效应显著, 本文提出一种二维、二区、二流体数学解析模型, 进一步研究IAFB的传热过程。

二、物理模型

2.1 可视化实验

作者曾经进行了IAFB的可视化系统研究^[4], 观察了液体过冷度, 加热热流率和质量流量对汽膜特征的影响, 图1(见10页)系三种典型结果, a、b、c三张照片上的液体入口过冷度分别为6、14和31°C。图1c表示, 自DNB截面处开始形成一等厚汽膜并向下游发展, 随后系一逐渐增厚的汽膜和汽-液波动界面, 图1b(见10页)等膜厚区比图1c短, 图1a几乎不存在等膜厚区。Elias和Chambre按瞬态实验提出存在二个不同几何构形的IAFB区, 毗邻淬冷前沿

本课题得到国家教委科学基金资助。

下游为第一区，其特征为加热面和液芯之间为一交界面光滑的汽膜隔开。随后为第二区，其交界面呈不稳定波状。他们认为等膜厚的第一区意味着蒸汽完全由入口处形成，即在DNB截面区产生，交界面当场温度尚处于稍过冷状态。而膜厚渐增的不稳定波状汽-液交界面区表示自下游某一断面处液芯开始汽化，第一和第二区间的过渡条件可以认为液相达到当场饱和温度。根据我们的可视化实验照片可以推断，第一区是否发生与入口过冷度，加热热流率和质量流率有关。一般地说，在低过冷度和饱和入口工况下，仅发生第二区。

2.2 简化物理模型

图2(见10页)系根据可视化实验结果提出的一种简化IAFB双区模型。事实上，第一区内蒸汽受热汽膜应稍有增加(当然与系统压力有关)。但是，一旦交界面温度超过当场饱和温度便会过渡到第二区。在第二区内，因界面液体汽化汽膜便迅速增厚，在第一区内，总加热热流中的小部分用于使汽膜升温，而大部分用于减小液芯过冷度。在第二区内则部分热流用于液芯汽化，部分用于蒸汽升温。因而作者的双区模型强调热流体动力特性，而不仅是一种几何构形简化。模型仍然假定汽液交界面光滑，但认为膜厚是可以变化的。为了导出简化的微分守恒方程组，采用下述假定。

- (1) 在第一区内忽略液体汽化，汽化仅发生在第二区内。
- (2) 蒸汽环膜完全将加热面与液芯隔开，液芯内无汽泡，汽膜内无液滴夹带。
- (3) 轴对称环状汽膜和液芯。
- (4) 两相压力相等，忽略因交界面汽化推力对两侧压力的影响。
- (5) 紊流蒸汽膜和紊流液芯流动。
- (6) 汽膜不接受辐射加热。
- (7) 定常流动。

三、数学模型

前面已经指出在IAFB区内，随着流动向下游推进和热量输入，蒸汽膜逐渐增厚。新增的汽膜和渐缩的液芯导致汽膜速度分布形状和液芯速度分布形状不断变化，速度变化影响到两相的温度分布不断变化，形成一种热入口区问题。二维效应显著，有必要讨论其影响。现将二维、二区、二流体数学模型简述于下。

3.1 守恒方程组

在二维、二区、二流体假定下，汽膜和液芯的质量、动量、能量守恒方程分别是

$$\frac{\partial}{\partial z}(\rho V_z) + \frac{1}{r} \frac{\partial}{\partial r}(r \rho V_r) = 0 \quad (1)$$

$$\rho V_r \frac{\partial V_z}{\partial r} + \rho V_z \frac{\partial V_z}{\partial z} = -\frac{dp}{dz} - \rho g + \frac{1}{r} \frac{\partial}{\partial r}(\mu r \frac{\partial V_z}{\partial r}) \quad (2)$$

$$\rho C_p (V_r \frac{\partial T}{\partial r} + V_z \frac{\partial T}{\partial z}) = \frac{1}{r} \frac{\partial}{\partial r}(K r \frac{\partial T}{\partial r}) \quad (3)$$

在导出上述方程过程中忽略了粘性耗散和比较小的项。此外，相变方程为

$$\frac{d}{dz} \int_0^{R_1} \rho_v V_z 2\pi r dr = -I', \quad (4)$$

$$\frac{d}{dz} \int_{R_1}^R \rho_l V_z 2\pi r dr = \Gamma, \quad (5)$$

这里下标v指蒸汽相，l指液相。将方程(4)和(5)相加后有积分式

$$\int_0^{R_1} \rho_v V_z 2\pi r dr + \int_{R_1}^R \rho_l V_z 2\pi r dr = W = \text{总质量流量}$$

3.2 边界条件

壁面处边界条件为

$$\begin{aligned} V_r|_{r=R} &= 0 \\ V_z|_{r=R} &= 0 \\ (K \frac{\partial T}{\partial r})|_{r=R} &= q_w - q_r \end{aligned} \quad (6)$$

式中 q_r —— 辐射热流分量；

q_w —— 总加热热流。

汽-液交界面处的交界条件为

$$\begin{aligned} V_{z,v}|_{r=R_1} &= V_{z,l}|_{r=R_1} \\ (\mu \frac{\partial V_z}{\partial r})|_{r=R_1} &= (\mu \frac{\partial V_z}{\partial r})|_{r=R_1} \end{aligned} \quad (7)$$

$$T_v|_{r=R_1} = T_l$$

$$\Gamma_l = \frac{2\pi R_1}{H_{l,v}} \left[(K \frac{\partial T}{\partial r})|_{r=R_1} - (K \frac{\partial T}{\partial r})|_{r=R_1} + q_r \frac{R}{R_1} \right]$$

在第一区内交界面的液侧传递的热量全部用于减小液芯过冷度，因而

$$(K \frac{\partial T}{\partial r})|_{r=R_1} = (K \frac{\partial T}{\partial r})|_{r=R_1} + q_r \frac{R}{R_1} \quad (8)$$

但是，在第二区内假定了交界面处于饱和状态，于是

$$T_l|_{r=R_1} = T_s \quad (8a)$$

在液芯轴线处，因对称而有边界条件

$$\begin{aligned} V_r|_{r=0} &= 0 \\ \frac{\partial V_z}{\partial r} \Big|_{r=0} &= 0 \\ \frac{\partial T}{\partial r} \Big|_{r=0} &= 0 \end{aligned} \quad (9)$$

3.3 初始条件

如果在DNB处的初始流动参数值已知，或者给定计算式，那么便可用有限差分方法数值

求解守恒方程组。

3.3.1 温度和质量流率

按照Elias的假定, 初始温度分布为

$$T_v(r, 0) = T_1 \quad (10)$$

蒸汽膜和液芯的初始流率为

$$W_{v,0} = \frac{Q_{Hv}}{H_g - H_l} \quad (11)$$

$$W_{l,0} = W - W_{v,0}$$

式中 Q_{Hv} 为热块处用于产生蒸汽的部分热量, 如果热块总加热量为 Q_H , 则有

$$H_{l,0} = H_l + \frac{Q_H - Q_{Hv}}{W_{l,0}} \quad (12)$$

于是液相的初始温度应为

$$T(r, 0) = T_{l,0} = f(H_{l,0})$$

3.3.2 速度分布

通常, 发生DNB之前流动处于旺盛状态, 假定液芯的初始速度分布为均匀分布, 即

$$V_{l,0}(r, 0) = V_{l,0} = \frac{W_{l,0}}{\rho_{l,0} \pi R_0^2} \quad (13)$$

R_0 是初始液芯半径。一般初始汽膜处于层流流动, 假定为抛物型分布, 即

$$V_{v,0}(r, 0) = A_2(R-r)^2 + A_1(R-r) \quad (14)$$

式中

$$A_2 = \frac{2V_{l,0}\rho_v\delta_0(3R-2\delta_0) - 6W_{v,0}}{\rho_v\delta_0^3(2R-\delta_0)}$$

$$A_1 = (V_{l,0} - A_2\delta_0^2)/\delta_0$$

δ_0 为初始汽膜厚度, 其值为 $\delta_0 = R - R_0$, 可以用相变方程计算。 δ_0 取值对壁温的影响不大, 后面将进一步论证。

3.3.3 初始蒸汽含汽率

初始平衡含汽率 $X_{e,0}$ 和真实含汽率 $X_{r,0}$ 分别为

$$X_{e,0} = (H_l + \frac{Q_H}{W} - H_l)/H_l \quad (15)$$

$$X_{r,0} = W_{v,0}/W$$

沿途含汽率是z-变量, 因而均匀加热条件下有

$$X_r(z) = X_{r,0} + \frac{q_w \cdot z}{W \cdot H_{fg}} \quad (16)$$

$$X_e(z) = X_{e,0} + \frac{1}{W} \int_0^z \Gamma_r(z) dz \quad (17)$$

于是真实空泡率 $\alpha(z)$ 为

$$\alpha(z) = 1 - \frac{R_1^2}{R^2} \quad (18)$$

3.4 本构方程式

为构成完全方程组, 必须确定粘度和热导率本构方程式, 令

$$\begin{aligned}\mu &= \mu_L + \epsilon_m \cdot \rho \\ k &= k_L + \epsilon_h \cdot \rho C_p\end{aligned}$$

式内 μ_L 和 k_L 系指层流粘度和层流热导率, ϵ_m 和 ϵ_h 系指动量涡团扩散率和能量涡团扩散率。 μ_L 和 k_L 与当场温度和压力条件有关, ϵ_m 和 ϵ_h 与当场流体动力状态和位置有关。若认为普朗特混合长度原理适用,则动量传递的涡团扩散率为

$$\epsilon_m = cl(\bar{V}_{m,1} - \bar{V}_{m,0})$$

这里 l 是指混合长度, c 是比例常数。按照Fung的假定^[5]将混合长度定义为紊流蒸汽膜厚度之半 $\delta(z)/2$ 。此外,括号内的速度差假定与平均液相速度成比例,即液相 ϵ_{m1} 为

$$\epsilon_{m1} = c_1 \left(\frac{1}{2}\delta\right) \bar{V}_{z1} \quad (19)$$

\bar{V}_{z1} 是液芯平均速度。对于汽膜,假定混合长度比例于计算点与壁面之间的距离

$$\epsilon_{m,r} = c_r (R-r) \bar{V}_{r,r} \quad (20)$$

对于热涡团扩散率,假定用下式计算紊流普朗特数 $Pr_{t,r}$,

$$Pr_{t,r} = \epsilon_{m,r} / \epsilon_h$$

如果认为Reynold相似适用,则 $Pr_{t,r} = 1$,于是汽膜可采用Webb的修正关系式^[6],

$$Pr_{t,r} = \frac{1 + 57 Re_r^{-0.45} \cdot Pr_{t,r}^{-0.61} \cdot \exp\left[-\left(\frac{R-r}{R}\right)^{\frac{1}{2}}\right]}{1 + 135 Re_r^{-0.45} \cdot \exp\left[-\left(\frac{R-r}{R}\right)^{\frac{1}{2}}\right]} \quad (21)$$

为了简化计算,采用Fung的分析,取 c_1 为0.08。按照Stewart的实验数据^[6], $Pr_{t,r}$ 在0.55~0.65之间,本分析采用0.6。调整参数 c 为0.17。于是各本构关系式近似为

$$\begin{aligned}\mu_1 &= \mu_{L1} + 0.04 \delta \cdot \bar{V}_{z1} \rho_1 \\ k_1 &= k_{L1} + 0.04 \delta \cdot \bar{V}_{z1} \rho_1 C_{p1} \\ \mu_r &= \mu_{Lr} + 0.017 (R-r) \bar{V}_{r,r} \cdot \rho_r \\ k_r &= k_{Lr} + 0.0283 (R-r) \bar{V}_{r,r} \cdot \rho_r \cdot C_{pr}\end{aligned} \quad (22)$$

3.5 热流率关系式

一个好的IAFB机理模型应当真实地模拟所涉及的各种传热机理,按目前研究状况,人们对涉及的传热过程尚了解不多,尚属一待开发的领域。按照前述讨论并结合假定6可以使用下述关系式计算管壁与液芯之间的辐射换热 q_R

$$q_R = \frac{\sigma_{0.95}}{\frac{1}{\epsilon_w \sqrt{1-\alpha}} + \left(\frac{1}{\epsilon_1} - 1\right)} \left[(T_w + 273.15)^4 - (T_{|r=r_1} + 273.15)^4 \right] \quad (23)$$

这里, $\sigma_{0.95}$ 为斯蒂芬-玻耳兹曼常数, ϵ 为辐射率。

实际上,汽-液交界面随机扰动会使液芯与加热表面发生间断性接触,即随机地润湿加热表面,Edelman^[7]的实验表明,在临界后IAFB的初始段内表面再润湿明显可见,它与液体入口过冷度有关,再湿概率可高达80%,并自DNB截面向下游按指数律衰减。因此,关系(22)应修正为

$$k_r = k_{Lr} + \epsilon_r \rho_r C_{pr} + C_1 [\exp(C_2 (T_w - T_{|r=r_1})) - 1] \cdot k_{Lr}$$

对于入口为过冷状态的IAFB工况,IAFB将在DNB截面下游一定距离处过渡为块状流或弥散流,但IAFB区终止或液芯碎裂的机理很不清楚,文献中有几种假定。Groeneveld认为,

当空泡率 $\alpha > 30\%$ 后自IAFB过渡为块状流; Analytis和Yadigaroglu假定大幅度交界面波是导致液芯碎裂的原因,使用临界韦伯数估计,但是临界韦伯数值至今无准确数据。本文采用液芯中心轴处达到当场饱和温度,从而引起液体整体沸腾导致液柱碎裂作为过渡准则。在所有计算中按当场汽膜温度 $T_w(z)$ 计算全部蒸汽物性。

四、壁温估计和比较

作者选择Stewart的实验数据^[6]校验模型,所选择的数据范围为压力:2.3,4MPa;质量流速:210~295kg/(m²·s);加热热流率:120~250kW/m²;入口过冷度:12~46°C。绝大多数工况下,壁温估计值与实验结果相当一致,详细比较可参阅文献^[6]。168个壁温数据平均绝对偏差约13°C,相对偏差约2.27%,图3(见11页)系一些典型结果。图上实线是壁温计算值,虚线为Stewart数据拟合曲线。图4(见10页)为截面下游0.4m断面处的径向速度分布和温度分布。因蒸汽粘性小,热导率小,故两种分布在汽膜区变化剧烈。

过冷度和热流率对汽膜厚度的影响示于图5(见12页)。第一区汽膜厚度几乎不变或略有增大;第二区内,因液芯汽化膜迅速增厚,计算预示趋势与可视化观察一致。

在本模型分析中没有包括DNB起始点计算研究,目前也并不清楚DNB点参数如何影响径向温度分布形状。作者就不同的初始汽膜厚度选择来讨论其影响,其结果示于图6(见11页)。计算表明不同的初始汽膜厚度取值仅呈现一种初始扰动效应,且很快衰减。超过DNB下游3cm处后膜厚几乎不受不同初始值的影响,壁温变化也几乎不受影响。由此可以推论:初始条件对壁温的影响呈一种当场现象,仅在DNB下游范围内略有影响。

作者任选一个工况讨论了IAFB的流动二维效应。比较结果表明:在第一区内,二维效应极小,壁温绝对偏差 $\leq 1.5^\circ\text{C}$,相对偏差为0.25%;在第二区内影响大些,绝对偏差为6°C,相对偏差为0.8%。如果不考虑径向速度分布影响,则壁温计算值稍高。注意到模型中尚不得含有几个调整经验常数,则可以推论:忽略径向速度分量不会引起严重误差,反而可以大大减少计算时间和节约费用。

五、结 论

1、发展了一个二维、二区、二流体数学解析模型预测管内流动下逆环状流膜态沸腾传热的壁面温度。分析了各种参数对壁温变化的影响,计算结果与Stewart的实验数据相当一致。

2、为了估计二维效应,进行了一维对比计算。在第一区内,二维效应甚小,第二区稍大。对于壁温计算,不考虑二维效应计算值偏大,趋于保守。

3、初始条件仅对DNB截面下游毗邻区有影响,超过此区后膜厚计算值和壁温计算值都不受影响。

参 考 文 献

(见12页)



P.O.Box 2103

Beijing, China

China Nuclear Information Centre
